IEEE Access
Multidisciplinary ⋮ Rapid Review ⋮ Open Access Journal

Date of publication xxxx 00, 0000, date of current version xxxx 00, 0000.

Digital Object Identifier xx.xxxx/ACCESS.2019.DOI

Unobtrusive and Continuous BCG-based Human Identification Using A Microbend Fiber Sensor

YI ZHANG[1], (Member, IEEE), ZHIHAO CHEN[2], (Senior Member, IEEE), WEIJUAN CHEN[3], and HUI LI[4].

[1]Photonic Technology Research Center, Quanzhou Normal University, China (e-mail: yzhang.cn@outlook.com)
[2]Photonic Technology Research Center, Quanzhou Normal University, China (e-mail: zhihaochen@qztc.edu.cn)
[3]College of Photonic and Electronic Engineering, Fujian Normal University, China (e-mail: weijuanchen@outlook.com)
[4]College of Photonic and Electronic Engineering, Fujian Normal University, China (e-mail: hli1688@126.com)

Corresponding author: Zhihao Chen (e-mail: zhihaochen@qztc.edu.cn).

ABSTRACT Biometric-based human identification has been investigated and applied in daily life applications, but some of them meet fundamental limitations, e.g., highly sensitive to the ambient light of the image-based recognition and unable to detect wrinkle finger with the fingerprint identification, and therefore decrease the user experience. Recently, electrocardiogram (ECG) has demonstrated to be a very attractive identification technique against attacks. However, the ECG-based human identification is still not a convenient solution since direct skin-contact and chest/body hair shaving are required for ECG acquisition even with the novel single-lead ECG. We propose and experimentally demonstrate an unobtrusive and continuous ballistocardiogram (BCG)-based human identification system using a microbend fiber sensor, which provides a more convenient way to identify the human who is seating on the chair with leaning back against the specially-designed cushion. To the best of our knowledge, this is the first study that a microbend fiber sensor is exploited for human identification. The results show that the proposed 1D-convolutional neural network (CNN) delivers outstanding performance with an average 100% and 90% identification rate under 15 subjects and 30 subjects, respectively. We recommend that the BCG-based biometric identification technique has great potential to be an innovative solution in smart, private and security applications with a small group.

INDEX TERMS Ballistocardiogram (BCG), Human Identification, Microbend Fiber Sensor

I. INTRODUCTION

BIOMETRIC-BASED human identification is now gaining tremendous attention to meet increasing security and privacy requirements. A wide range of conventional biometric-based identification techniques have been investigated and applied in daily life applications, such as speech recognition, calligraphy recognition, fingerprint identification [1], iris recognition [2] and face recognition [3]. Moreover, gait recognition appears to be a promising technology at a low-resolution situation, i.e., low image quality or little image detail, where conventional biometric-based methods cannot be employed [4]. It has been proved that gait sequences can be captured and measured at a low-resolution situation while iris or face recognition could not work properly without high enough resolution [5]. We know that the image-based recognition is highly sensitive to the ambient light and even the widely used fingerprint identification meets the challenge with the dry or wet and wrinkled finger. What's more, those existing techniques are easy to be spoofed. For example, the fingerprint of a specific person can be collected and recreated using kids' modeling clay or latex. Face ID, a standout face recognition application supported by iPhone X, still can be fooled by identical twins. Those limitations of both fingerprint identification and face recognition techniques decrease the user experience in mobile and non-mobile applications, especially for smartphone unlocking. On the other hand, the conventional human identification, e.g., the fingerprint identification technique, which usually provides one-shot authorization in some private and security applications, may encounter illegal access once the administrator/possessor temporarily leaves without logging out. Nevertheless, the unobtrusive and continuous human identification, which is able to unobtrusively, continuously identify human subjects without any inconvenience to the person being monitored, has potential to prevent this severe security risk by continuous identity authentication.

Heartbeat-based human identification has shown its robustness against attacks in recent years. A heartbeat is the physical contraction of the heart muscle caused by chemical/potential differences in the component cells called myocytes [6]. Different subjects have their individual heartbeat patterns due to the difference between age, gender, weight, cardiac structure, etc. The heartbeat performs as a unique life indicator to represent a subject and it is difficult to manipulate or replicate. Electrocardiogram (ECG), which reflects the cardiac electrical activity of the heart recorded by a set of electrodes placed on the body surface, has been widely used in clinical diagnoses and recently has demonstrated to be a very attractive technique in human identification [7]. However, ECG-based human identification has been restricted so far since the conventional ECG acquisition needs to attach multiple electrodes on the body surface, such as the traditional 12-lead configurations on the chest and two-wrist. A novel single-lead ECG has been presented recently as an alternative wearable solution to monitor dynamic ECG [8] but it still requires direct skin-contact. Moreover, chest/body hair needs to be shaved for some people to improve the ECG signal quality, which usually leads to inconvenience to the user.

Different from the conventional uncomfortable/inconvenient ECG systems, the ballistocardiogram (BCG) technique is a noninvasive method to monitor heart activity unobtrusively and continuously. Fundamentally, BCG [9] produces a graphical representation of repetitive motions of the human body arising from the sudden ejection of blood into the great vessels with each heartbeat [10]. Therefore, the heartbeat patterns hold in the BCG signal can be regarded as important indicators for biometric identification. Note that, the BCG measurement by piezoelectric (PZT) sensors [11] is the total applied force from the seating human body. The original acquisition signal must be interfered by talking, swallowing, respiration and other unnatural body movements, which poses challenges to BCG signal retrieval and BCG-based biometric identification. Moreover, it has been proved that the PZT effect is dependent on temperature [12] and the PZT sensors are vulnerable to electro-magnetic interference (EMI) [13], and therefore limits the identification accuracy. Nevertheless, the fiber optic sensors (FOSs) can achieve good electromagnetic compatibility (EMC) without any influence by temperature so as to provide highly sensitive and high precision BCG measurement [14].

In this paper, we propose and experimentally demonstrate an unobtrusive and continuous BCG-based human identification system using a microbend fiber sensor. We develop a smart cushion as a physiological monitor to capture the BCG signal of the subject leaning back against. Specifically, a microbend fiber sensor embedded into the cushion can provide continuous measurement to the body vibrations on the cushion including the heartbeat. To the best of our knowledge, this is the first study that a microbend fiber sensor is exploited for human identification. We perform a pre-processing operation to retrieve BCG signals from the original signal captured by the microbend fiber sensor, and then provide two feasible methods to effectively extract time domain BCG features basing on J-peak detection. In addition to the three general classification algorithms, we propose a 1-D convolutional neural network (CNN) to utilize the full timing information of BCG morphological structure. Specifically, the segment extracted by the proposed J-peak segmentation rather than simple blind segmentation [15] is fed into the 1D-CNN. The experimental results show that the filtered BCG signal apparently reveals the BCG pattern of the subject. The 1D-CNN shows the robust to the state variation of subjects, which delivers outstanding performance with an average 100% and 90% identification rate under 15 subjects and 30 subjects, respectively.

Note that biometric information is unique but not secret among individuals, all biometric-based human identifications are vulnerable to presentation attacks, which attempt to invade the system with an artifact or contraption. Vitality detection is a provable defense technique against the spoof attacks of a biometric system, which aims to detect whether the presented biometric sample is live or fake [16]. It has been claimed that the ECG offers inherent vitality detection, and therefore the ECG-based human identification is the robustness to presentation attacks [17]. Similarly, it can be proved that the inherent vitality detection is guaranteed in the BCG-based human identification (e.g., respiratory rate and heart rate can be measured from BCG signals). Therefore, the proposed BCG-based human identification can provide a high degree of security and privacy authorization.

Our main contributions are as follows.

- An unobtrusive and continuous BCG-based human identification system is proposed and experimentally demonstrated without the need of additional ECG data acquisition. Compared with the ECG-based identification, the proposed BCG-based identification system provides a more convenient way to identify the human who is seating on the chair with leaning back against the specially-designed cushion.
- This is the first study that a microbend fiber sensor is used for unobtrusive and continuous BCG-based human identification. Compared with the PZT sensor, the proposed optical sensor has good electromagnetic compatibility and therefore can improve the identification accuracy through highly sensitive and high precision BCG measurement.
- The inherent vitality detection of the BCG can offer a high degree of security and privacy authorization against the spoof attacks. The experimental results confirm that the proposed biometric identification technique has great potential to be an innovative solution in smart, private and security applications with a small group.

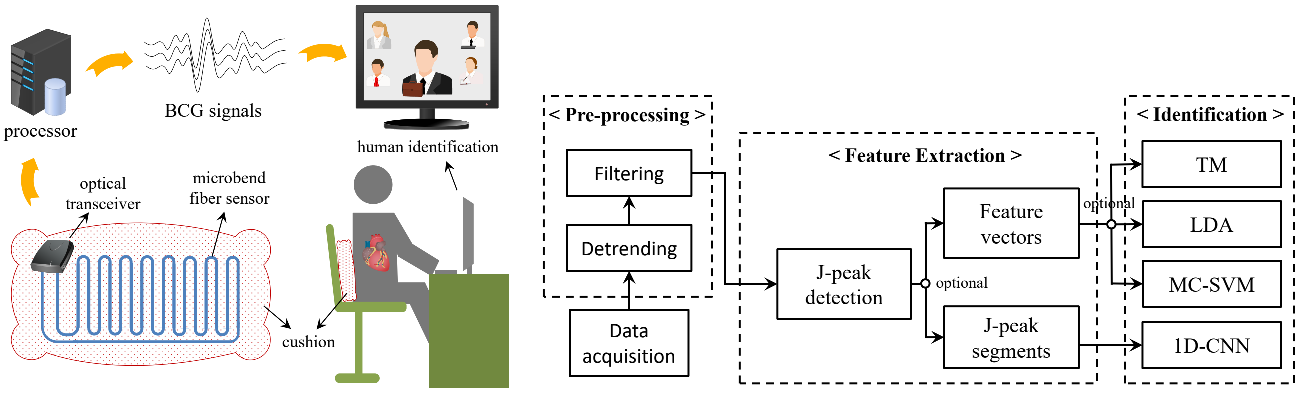

(a) System architecture

(b) System diagram

FIGURE 1: Proposed continuous human identification system

A. RELATE WORK

Several algorithms have been developed in the literature for ECG-based human identification [7], [15], [18]–[20]. Time domain ECG features, saying the normalized distance between the two fiducials, are identified from P, R, and T complexes to identify individuals [18]. Specifically, the locations of fiducial points are determined by tracking downhill and meanwhile minimizing the radius of curvature. To improve the identification accuracy, two feature extraction methods, principal component analysis (PCA) and kernel principal component analysis (KPCA), are combined with a single binary classifier of support vector machine (SVM) [19]. In addition, CNN is one of the main-stream deep learning algorithms in many classification and recognition applications, especially for biometric-based human identification. A multiresolution CNN architecture [15] is proposed to provide automatic feature learning and human identification from wavelet domain ECG streams. To avoid heavy fiducial point detection, a blind segmentation is applied and further auto-correlation is operated to remove the phase difference. Besides, the CNN is used to identify individuals from weak ECG acquired by both single-arm-ECG and ear-ECG [20]. Specifically, by using state space reconstruction, ECG heartbeats are projected to suitable 2D images which serve as the input for CNN to reveal heartbeats' trajectory behaviors. However, the conventional ECG acquisition needs to attach multiple electrodes on the body surface, such as the traditional 12-lead configurations on the chest and two-wrist. Although non-standard convenient ECG lead configurations, e.g., single-arm-ECG lead [20] and novel single-lead ECG [8], have been provided to the long-term wearable applications, it is still not a convenient solution for human identification since direct skin-contact and chest/body hair shaving are required. Inversely, the BCG technique provides unobtrusive and convenient signal acquisition for human identification.

The feasibility of BCG for human identification is firstly investigated by the state-of-the-art research [11] by using correlation analysis of BCG segments. To partition each BCG segment into epochs associated with the cyclical R peak of ECG, it requires simultaneous BCG and ECG data acquisition. In our system, single information of BCG signal is required rather than the cooperation between BCG and ECG [11]. We develop a microbend fiber sensor to capture the BCG signal of the subject. Moreover, we know that the data acquisition of BCG signal depends on the measurement of heartbeat induced body vibrations accompanied by talking, swallowing, respiration and other unnatural body movements from the subject. This poses challenges to BCG signal retrieval and BCG-based biometric identification. In the state-of-the-art research [11], the BCG signal is obtained from a measurement chair installed three PZT sensors. Note that the PZT sensor is an electrical sensor, which is temperature-dependent [12] and is also inevitably susceptible to electromagnetic disturbance [13], therefore, the operating environment, as well as the identification performance, is restricted for the practical applications. However, the specially-designed cushion in our system is embedded with a microbend fiber sensor, which is an optical sensor solution to provide highly sensitive and high precision BCG measurement [14]. Note that both the PZT sensor and the proposed optical sensor suffer severe noise interference to the fundamental signal frequency. Nevertheless, higher order harmonics of the BCG signal are rarely interfered in the proposed optical sensor and therefore benefits to the BCG signal reconstruction against noise [21].

II. METHODS

As illustrated in Fig. 1(a), the proposed human identification system based on BCG signals using microbend fiber sensor can continuously identify the human who is seating on the chair with leaning back against the specially-designed cushion. Note that, the BCG information of a specific human should be recorded before the identification process starts. In the traditional ECG system, ECG signal is recorded by attaching a set of electrodes on the body surface, such as

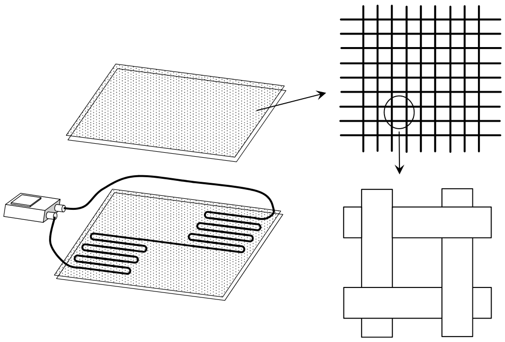

(a) Sensor inside smart cushion

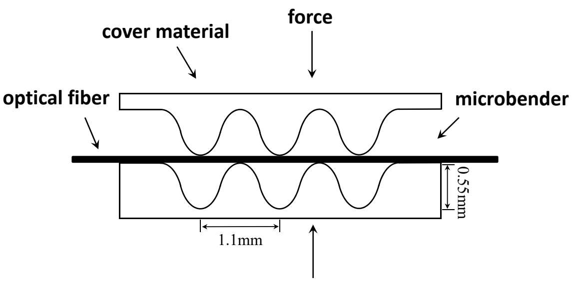

(b) Sensor inside handheld module

FIGURE 2: Schematic of the microbend fiber sensor

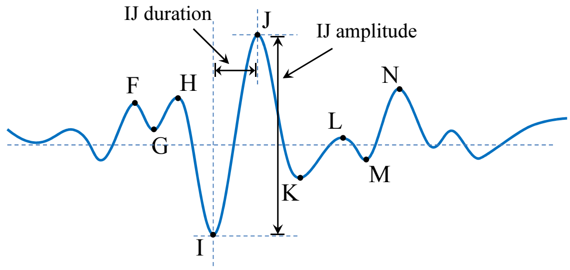

FIGURE 3: A typical BCG waveform of the normal human subject

TABLE 1: Selected features used for identification

Total 16 selected features		
1. FG amplitude	7. IJ amplitude	13. LM amplitude
2. FG duration	8. IJ duration	14. LM duration
3. GH amplitude	9. JK amplitude	15. MN amplitude
4. GH duration	10. JK duration	16. MN duration
5. HI amplitude	11. KL amplitude	
6. HI duration	12. KL duration	
Hints: "a" = amplitude	"d" = duration	

the neck, chest, arms, legs, etc. However, BCG signal in our setup is captured by a smart cushion, which can be regarded as a non-wearable physiological monitor that simultaneously detects heartbeat, respiration, BCG waveform and body movement. Specifically, a microbend fiber sensor [22] using multi-mode optical fiber is embedded into the cushion. The proposed microbend fiber sensor is shown in Fig. 2(a), where a section of graded multi-mode optical fiber is clamped between a pair of microbenders (pressure plates). To improve its sensitivity compared with our previous work, we use a novel material with mesh structure as the microbender of the proposed microbend fiber sensor in Fig. 2(a). The sensor connected to an optical transceiver is highly sensitive to the applied force and low cost. The optical transceiver consists of a light source, a detector, a microprocessor and other circuits for noise floor reduction. Basing on microbending fiber optic theory, the body vibrations on the cushion including the heartbeat is presented as the microbend loss effect of light through the fiber measured by the transceiver. Furthermore, to confirm the possibility of the proposed BCG-based human identification system in mobile applications, we provide a handheld module using a microbend fiber sensor. For the handheld application, microbend fiber based hand sensor must be very small. We designed a pair of microbenders where the period of the tooth spacing was 1.1mm and only 3 periods were used as shown in Fig. 2(b). The overall system diagram is shown in Fig. 1(b).

A. PRE-PROCESSING OPERATION

The original BCG signal captured by the smart cushion is sampled at 50Hz and then transmitted to the processor through Bluetooth. Note that the measurement of the optical transceiver is the total applied force on the cushion, the original BCG signal must be interfered by talking, swallowing, respiration and other unnatural body movements. Therefore, we perform a pre-processing operation to retrieve the actual BCG signal. Firstly, the linear trends of the original signal are removed using the least-squares straight-line fit. Afterward, band-pass, low-pass and high-pass filter operations are sequentially employed to the detrending signal X implementing "Direct Form II Transposed" formulated as the following rational transfer function in the Z-transform domain:

$$Y(z) = \frac{B(1) + B(2)z^{-1} + \cdots + B(n_b+1)z^{-n_b}}{1 + A(2)z^{-1} + \cdots + A(n_a+1)z^{-n_a}} X(z), \tag{1}$$

where A and B are the denominator coefficient and numerator coefficient vectors, respectively. n_a and n_b are the feedback and feedforward filter order, respectively.

B. BCG FEATURE EXTRACTION

To effectively identify human subjects, the BCG heartbeat patterns need to be better studied. For time domain ECG signal, the features can be extracted by its wave shape, peak amplitude, point-to-point interval, etc. The QRS complex is widely used to describe the ECG heartbeat pattern [18]. To extract the features that represent the morphological structure of the BCG signal of different subjects, we share a similar

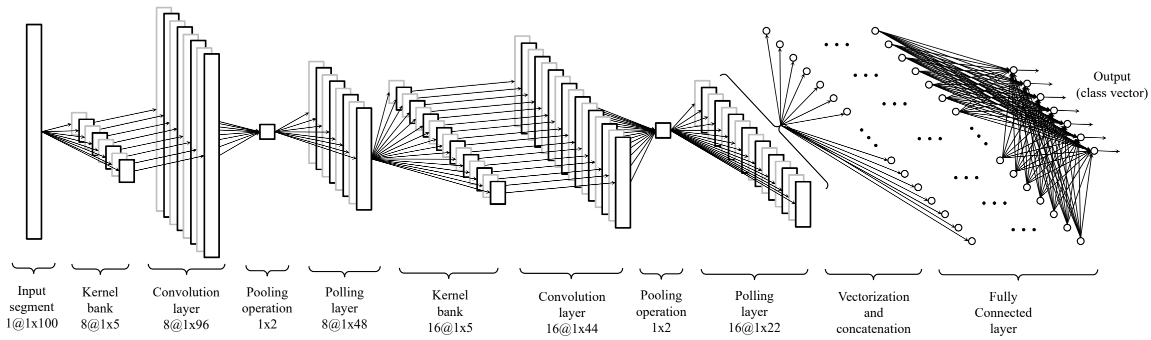

FIGURE 4: The architecture of 1D-CNN based identifications

idea by applying a fiducial method basing on the characteristic points of BCG waveforms. A typical BCG waveform of a normal human subject is shown in Fig. 3 with some fiducial points marked. We observe that J peak is the key feature of a typical BCG waveform. Specifically, we define IJ duration as the time delay between I point and J point. In addition, IJ amplitude is defined as the amplitude from point I to point J. We select 16 feature parameters concatenated as a feature vector as shown in Table 1, which consists of both duration and amplitude of any two adjacent fiducial points. We define the dataset of extracted features vectors as $\mathbf{X} = \{X_i^{(p)}\}$, $X_i^{(p)} = (x_{i,1}^{(p)}, \cdots, x_{i,16}^{(p)})$, $\forall p \in [1, M]$, $\forall i \in [1, N^{(p)}]$, where $X_i^{(p)}$ is i-th feature vector of subject p and M is the number of subjects. $N^{(p)}$ is the number of feature vectors of subject p such that $N = \sum_{p=1}^{M} N^{(p)}$ is the total number of feature vectors. A 0-1 normalization is further performed for each extracted feature vector to meet the input requirement of identification algorithms. Specifically, the BCG trace fiducial position is located by J-peak detection, which is beyond the scope of this paper, as some detection algorithms have been reported in the literature [23], [24].

Note that the above-extracted feature vector holds only basic characteristics of BCG waveform and may lose some useful timing information to support high accuracy identification. Moreover, the location of those fiducial points could not be correctly tracked due to heartrate variability (HRV). Therefore, we provide another method, called *J-peak segmentation*, to keep the full information of BCG morphological structure. We divide the BCG signal into individual segments based on the localization of the J wave peak so that each segment has an equal number of samples at each side of the J (center) point. Since the typical range of heart rate is from 40 to 208 beats per minute, we choose 50 (1 second) samples at each side of the center point. Specifically, 1 sample from the right-hand side is removed to satisfy the input of later 1D-CNN identification. In this way, we have a total of 100 samples in each segment. The J-peak segments are denoted by $\mathbf{S} = \{S_i^{(p)}\}$ for $\forall p \in [1, M]$ and $\forall i \in [1, N^{(p)}]$, as the BCG features for later identification.

C. HUMAN IDENTIFICATION

We find out that our human identification problem actually is a multi-class classification problem. To fast verify the potential of BCG-based human identification using the proposed feature extraction methods, three general classification algorithms are provided as follows:

1) Template Matching (TM)

Since different subjects have their individual heartbeat patterns represented by their BCG feature vectors, we consider to use template vector to classify each subject. For subject p, we propose an iterative approach to generate his/her template vector $V^{(p)} = (v_1^{(p)}, \cdots, v_{16}^{(p)})$, which is calculated by element average of his/her BCG feature vectors, $v_j^{(p)} = \frac{1}{N^{(p)}} \sum_{i=1}^{N^{(p)}} x_{i,j}^{(p)}, \quad \forall j \in [1, 16]$. Furthermore, we define the distance between the vector $X_i^{(p)}$ and the template $V^{(p)}$ by mean-squared error (MSE) $d_i = \frac{1}{16} \sum_{j=1}^{16} (x_{i,j}^{(p)} - v_j^{(p)})^2$. In each iteration, we remove the vector $X_{max}^{(p)}$, which has maximum distance d_{max}, from further calculation and then update $V^{(p)}$ by element average. The approach terminates once d_{max} is smaller than a predefined threshold d_{th}. Finally, we obtain a set of template vectors $\mathbf{V} = \{V^{(p)}\}$, $p \in [1, M]$. Similarly, we extract a test vector $V^{(test)}$ from the input testing BCG signal. Our template matching method is very simple that we compare MSE between $V^{(test)}$ and $V^{(p)}$ one-by-one and predicate the identity of the current test subject as p^* with minimum MSE.

2) Linear Discriminant Analysis (LDA)

LDA is a commonly used technique in pattern recognition to find a linear combination of features that separates two or more classes of objects. Different from principal component analysis (PCA), which is a unsupervised dimension reduction to feature classification and ignores class labels, LDA is a better choice for multi-class dataset since it maximizes the ratio of between-class variance to within-class variance in the dataset thereby guaranteeing maximal class separability. Therefore, we perform LDA as a subject classifier. The between-class scatter matrix $\mathbf{S}_b$ is computed as $\mathbf{S}_b = \sum_{p=1}^{M} N^{(p)}(\overline{X}^{(p)} - \overline{X})(\overline{X}^{(p)} - \overline{X})^{\mathrm{T}}$, where $\overline{X}^{(p)}$

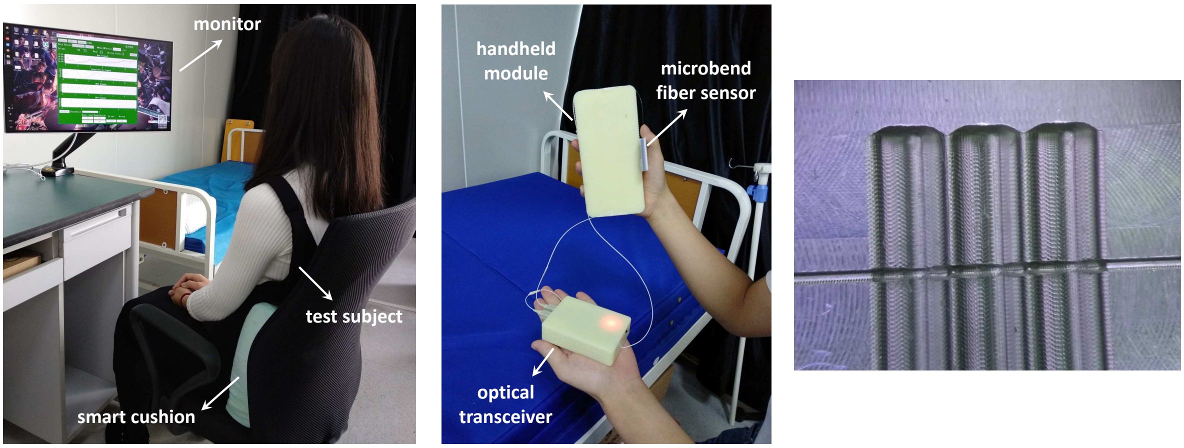

(a) Setup with smart cushion (b) Setup with handheld module (c) Metal microbender under the microscope

FIGURE 5: Experimental setup of the human identification system using a microbend fiber sensor

is the mean vector of class p and $\overline{X}$ is the mean vector of full dataset $\mathbf{X}$. The within-class scatter matrix $\mathbf{S}_w$ is calculated as $\mathbf{S}_w = \sum_{p=1}^{M}\sum_{i=1}^{N^{(p)}}(X_i^{(p)} - \overline{X}^{(p)})(X_i^{(p)} - \overline{X}^{(p)})^{\mathrm{T}}$. Finally, the LDA coefficient matrix $\mathbf{W}$ is obtained by $\mathbf{W} = \underset{\mathbf{W}}{\arg\max}(\mathbf{W}\mathbf{S}_w\mathbf{W}^{\mathrm{T}})^{-1}(\mathbf{W}\mathbf{S}_b\mathbf{W}^{\mathrm{T}})$. When we try to identify a subject, a linear score matrix $\mathbf{G}$ can be calculate by $\mathbf{W}^{\mathrm{T}}\mathbf{X}^{(test)}$, where $\mathbf{X}^{(test)}$ is the feature vector set of this testing subject. Note that, each column of $\mathbf{G}$ represents the score for each class. That is, higher score the class achieves, more likely the subject belongs to that class.

3) Multi-class Support Vector Machine (MC-SVM)

The solution of binary classification problems using SVM is well developed. To extend it to multi-class scenario, several methods have been proposed, such as "one-against-all", "one-against-one" and directed acyclic graph SVM (DAGSVM) [25]. We use one-against-one method, which is also known as "pairwise coupling", to construct a MC-SVM by multiple binary classifiers, where each one is trained to distinguish the feature vectors of one class from another class. A MC-SVM is constructed by combining $M(M-1)/2$ binary classifiers, where each one is trained to distinguish the feature vectors of one class from another class. Given total N vectors $(X_i, y_i), i = 1, \cdots, N$, where $X_i \in \mathbf{X}$ and $y_i \in [1, M]$ is the class of X_i. Then, the binary classification problem for the training vectors from subject p and subject q is as follows:

$$\begin{gathered}\min_{w^{pq}, b^{pq}, \xi_i^{pq}} \frac{1}{2}(w^{pq})^{\mathrm{T}} w^{pq} + C\sum \xi_i^{pq}(w^{pq})^{\mathrm{T}} \\ (w^{pq})^{\mathrm{T}}\phi(X_i) + b^{pq} \geq 1 - \xi_i^{pq} \text{ if } y_i = p, \\ (w^{pq})^{\mathrm{T}}\phi(X_i) + b^{pq} \leq -1 + \xi_i^{pq} \text{ if } y_i = q, \\ \xi_i^{pq} \geq 0, \end{gathered} \tag{2}$$

where C is the penalty parameter of the error term and the vector X_i is mapped to a higher dimensional space by the function ϕ. After trying difference kernel types, we finally select polynomial kernel function $K(X_i, X_j) = (\gamma X_i^{\mathrm{T}} X_j + r)^d \equiv \phi(X_i)^{\mathrm{T}}\phi(X_j)$. We use voting strategy for future identification. That is, the class predicted by each SVM classifier gets a vote. At last, we predict the class with largest votes as the identification result.

D. 1D-CONVOLUTIONAL NEURAL NETWORK (1D-CNN)

CNN [26] has shown impressive performance in many classification and recognition applications, especially widely used for 2D image classification. We implement 1D-CNN to utilize the features extracted from J-peak segmentation in this section. As shown in Fig. 4, the input of proposed 1D-CNN can be seen as a 1D-image (single-row image). There are two convolution layers and each one is formed by sliding different kernels (feature detectors) over the images of its previous layer without zero padding on the boundaries. Specifically, the kernel bank with size 5 is consist of 1D arrays (1x5) rather than 2D matrices in traditional CNN models. We define w_{ij}^{l-1} as the kernel bank from the ith neuron at layer $l-1$ to the jth neuron at layer l. Therefore, the convolution operation can be expressed as:

$$s_j^l = b_j^l + \sum_{i=1}^{N^{l-1}} conv1D(w_{ij}^{l-1}, o_i^{l-1}), \tag{3}$$

where N^{l-1} is the number of neurons at layer $l-1$, o_i^{l-1} is the output of the ith neuron at $l-1$th layer, s_j^l and b_j^l are the input and the bias of the jth neuron at layer l, respectively. To avoid overfitting, an average polling operation (downsampling) is carried out to reduce the size of images after each convolution layer and its output images form a polling layer. Furthermore, the images in the last polling layer are stretched to signal column vector and fed into the fully connected layer. Note that, the activation function, which defines the output of a neuron for both convolution layers and the fully connected layer is chosen as 'sigmoid'. When we feed the segments (1x100) extracted by J-peak segmentation into the 1D-CNN,

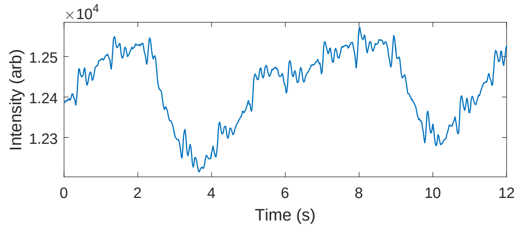

(a) Original BCG signal

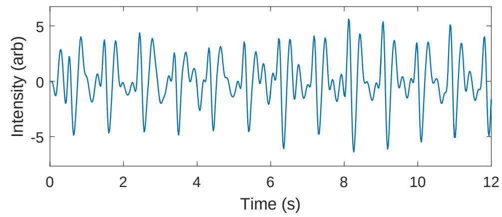

(b) Filtered BCG signal

FIGURE 6: Pre-processing operation to the captured BCG signal in continuous 12 seconds

the output class vector indicates the final identification result.

To effectively train the proposed 1D-CNN, we use the back-propagation (BP) approach [27] to update the parameters such as weight and bias. By the derivative of MSE loss function, which is the measured error between the actual and predicted value, we apply the gradient descent method to minimize this loss. Accordingly, a chain rule of the derivatives is performed to update the rest of the network parameters. To further accelerate the training process, we adopt a mini-batch training strategy for the total input segments. We define two stopping criterion of the training process: 1) a minimum training error lever that is set to 5%, and 2) a maximum number of BP epochs that is set to 2000. Note that some of the captured BCG signals may be messy signals due to the lower power of BCG signal interfered by other body movements, which will be discussed in the experimental results later. The blind segmentation has a high probability to generate non-BCG segments (mainly contain messy signals) and therefore will introduce bad inputs to the training process. However, the proposed J-peak segmentation provides a good way to find BCG segments and meanwhile reject bad inputs before fed into the 1D-CNN.

III. EXPERIMENTAL RESULTS

The experimental setup with both the smart cushion and the handheld module is shown in Fig. 5. Note that the outline of the handheld module in Fig. 5(b) is similar to the appearance of the mobile phone. For mobile applications, although the current light source and detector module we used in the experiment are big, they can be reduced to 2mm in diameter in the future. In the experiment, conventional 62.5micron multimode fiber was used. The metal microbender of the handheld module is observed under the microscope in Fig. 5(c).

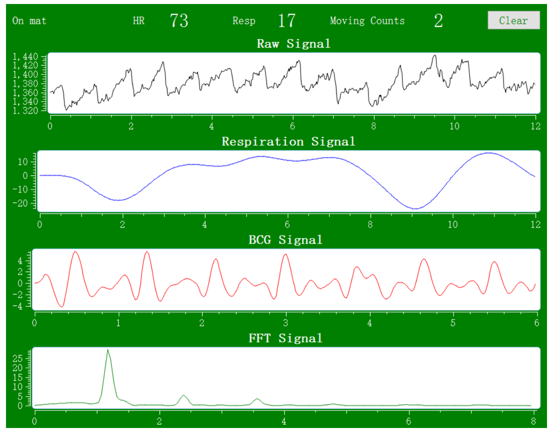

FIGURE 7: Real-time monitoring results with handheld module

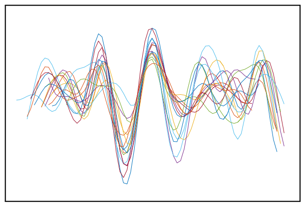

(a) Subject A

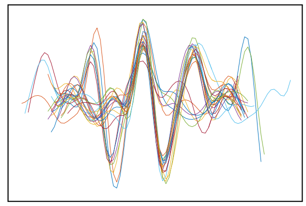

(b) Subject B

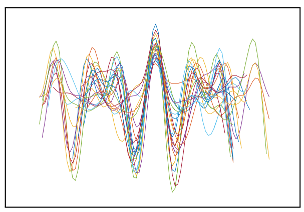

(c) Subject C

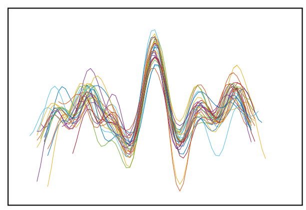

(d) Subject D

FIGURE 8: BCG waveforms of different subjects captured in continuous 20 seconds

A. PRE-PROCESSING OPERATION

We employ the proposed pre-processing operation to the captured BCG signal of a subject in continuous 12 seconds and the results are demonstrated in Fig. 6. Since the original BCG signal in Fig. 6(a) has about two and half clear waveform in continue 12 seconds, the respiratory rate of this subject can be estimated as $(60 * 2.5/12) = 12.5$ breaths per minute. Furthermore, we observe that some lower intensity peaks over the waveform, which have near-equal time interval, are synchronous with the heartbeats of the subject, saying the actually BCG signal we expect. By operating the proposed pre-processing, we obtain the filtered BCG signal as shown in Fig. 6(b), which apparently reveals subject's BCG heartbeat pattern. We further roughly calculate the heart rate as $(60 * 13/12) = 65$ beats per minute (bpm). Moreover, promising results by holding the handheld module in hand is shown in Fig. 7, including raw signal and BCG signal. We observe that the specially-designed handheld module can effectively collect BCG signals of the subject. That is to say,

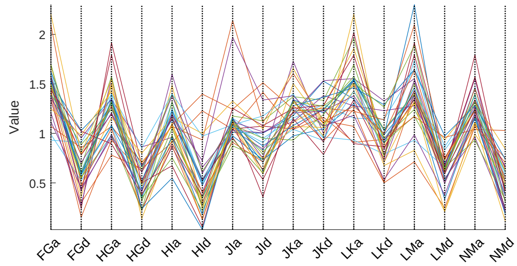

(a) Parallel coordinate display of Subject C

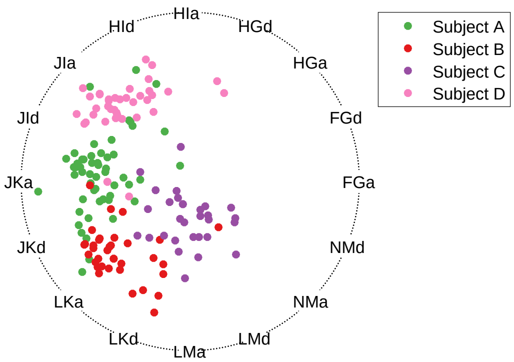

(b) RadViz display of different subjects

FIGURE 9: Feature vectors captured in continuous 60 seconds

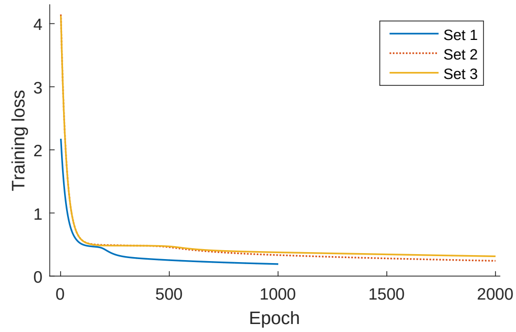

FIGURE 10: A Training process of the proposed 1D-CNN with epoch-loss

the proposed BCG-based human identification system also has potential in mobile applications.

B. BCG FEATURE EXTRACTION

We illustrate the BCG waveforms of four different subjects in Fig. 8 that captured in continuous 20 seconds basing on the J-peak detection. In each subfigure, e.g., Fig. 8(a), we observe that most of the waveforms follow a specific pattern, except for a small number of messy signals due to the lower power of BCG signal interfered by other body movements. It also shows the challenge and potential improvement about the data acquisition and signal processing of BCG information. In Fig. 8, we can recognize that different subjects own their individual BCG patterns. Moreover, the feature vectors of four subjects captured in continuous 60 seconds are shown in Fig. 9, where "a" and "d" represent the amplitude and the duration in Table 1, respectively. In Fig. 9(a), we find out that the extracted vectors of Subject C visualized using a parallel coordinate display hold the BCG pattern information to some extent, which motivates us to exploit a template vector to classify each subject. To enrich the differences among those subjects, radial coordinate visualization (Radviz) [28] is displayed in Fig. 9(b), which maps the attributes of feature vectors onto the surrounding circle and maps the feature points into the circle. We observe that the positions of feature points are scattered into four clusters, which represent those four subjects. However, the body actions cause some points deviated from their associated clusters so that there is no clear indication of the relations. The cluster centers can be used for identification, saying the template vector discussed above.

C. HUMAN IDENTIFICATION

To verify the performance of the proposed human identification system, we offline construct three datasets by collecting BCG information from the colleagues and students using the smart cushion:

- *Set 1*: 15 subjects (male/female: 10/5), age: 24 $\pm$ 5yrs, 1 minute training data, 20 seconds testing data;
- *Set 2*: 30 subjects (male/female: 18/12), age: 24 $\pm$ 5yrs, 1 minute training data, 20 seconds testing data;
- *Set 3*: 30 subjects (male/female: 18/12), age: 24 $\pm$ 5yrs, 5 minutes training data, 1 minute testing data.

Note that Set 2 and Set 3 have more subjects than Set 1. Compared with Set 2, Set 3 collects more BCG data of each subject for both training and testing processes. To validate the robustness of BCG data acquisition and the reliable of the normalized feature extraction, we purposely record the training data and the testing data with different leaning postures at different time points. In the training process, the training data is used to construct the identification model in different algorithms, e.g., to generate the feature vectors in TM. And then, we exploit the testing data in the identification process to correctly identify human subjects. In order to fit the real application scenario, each continuous test data for a subject, either 20 seconds in Set 1 or 1 minute in Set 2 and Set 3, is regarded as an independent test case. Afterward, we implement the proposed identification algorithms in MATLAB, respectively. Specifically, the implementation of the proposed MC-SVM bases on LIBSVM [29], which is an integrated software for support vector classification. LIBSVM provides different types of kernel function, including linear, polynomial, radial basis function, sigmoid and precomputed kernel. After repeated trials with different parameters, we find out that polynomial kernel function can achieve the best performance for our MC-SVM.

Table 2 shows the identification results. The accuracy is calculated as the number of correct identified subjects over the total number of subjects, and the overhead is estimated

TABLE 2: Identification Results

Method	Accuracy			Overhead		
	Set 1	Set 2	Set 3	Set 1	Set 2	Set 3
TM	86.67%	43.33%	50.00%	0.26s	0.47s	4.85s
LDA	93.33%	50.00%	66.67%	0.27s	0.65s	3.51s
MC-SVM	80.00%	43.33%	73.33%	0.42s	0.89s	41.76s
1D-CNN	100.00%	63.33%	90.00%	203.58s	670.78s	2188.23s

as the execution time of the training process. In general, Set 1 achieves the best accuracy, which means that the larger number of subjects increases the difficulty of successful identifications. The accuracy of Set 3 is higher than Set 2 since more BCG data is collected. For the three general classification algorithms, LDA shows better performance in Set 1 but its accuracy greatly decreases in Set 2 and Set 3. However, MC-SVM can achieve stable performance in both Set 1 and Set 3. The reason is that LDA is a linear classifier and has the poor ability when dealing with a big subject group, while the proposed MC-SVM is more flexible by adopting the polynomial kernel function with the extension of LIBSVM. We also observe that the three algorithms have low computational complexity and therefore the training overhead is negligible. To further promote the identification accuracy, we provide 1D-CNN, which utilizes the full BCG information by J-peak segmentation. As shown in Table 2, the proposed 1D-CNN can achieve 100% accuracy in Set 1, 63.33% accuracy in Set 2, and 90% accuracy in Set 3, which significantly outperforms the three general algorithms. The proposed 1D-CNN in Fig. 4 is a multi-layer and multi-neuron structure with different network parameters. To update those parameters that fitting the effective identification, it requires sufficient training data and BP training epochs. Therefore, the training overhead of 1D-CNN become larger than the general algorithms. A training process with epoch-loss is shown in Fig. 10. We find out that the training loss decreases with the training epochs, which means that the proposed BP approach is efficient to update the network parameters. Moreover, the training loss declines quickly and reaches the acceptable identification accuracy with only few dozen of epochs. The rest of the long epochs is optional to further increase the performance. We also observe that a smaller loss and faster training stable can be reached with a smaller number of subjects. Nevertheless, we recommend utilizing 1D-CNN to identify human subjects due to its impressive performance. In our future work, we expect to reconstruct the proposed 1D-CNN under some popular machine learning frameworks, i.e., TensorFlow, so as to reduce the training overhead with GPU acceleration.

IV. CONCLUSION

We recommend that the BCG-based biometric identification technique has great potential to be an innovative solution in smart, private and security applications with a small group. As the one-shot process in the conventional authorization (e.g., passwords, tokens or PINs), malicious people can illegally access highly sensitive information when the network administrator, who is designated to maintain computer infrastructures, temporarily leaves without logging out. Fortunately, our BCG-based human identification system provides continuous identity authentication to prevent this severe security risk in those conventional authorizations. Specifically, the proposed human identification can be employed in some military applications, where the continuous identify authentication is crucial when operating sensitive equipment. Moreover, we have experimentally confirmed the possibility of mobile applications by employing a specially-designed handheld module using a microbend fiber sensor. As the robustness against attacks of the heartbeat-based human identification, the proposed BCG-based human identification system stands a chance to be an alternative solution for smartphone unlocking and unobtrusive and continuous human identification.

ACKNOWLEDGMENT

This work was supported by the fund of Tongjiang Scholar Distinguished Professor and the fund of "Harbour Project" of Quanzhou under Grant 2017ZT013. It is also supported by Fujian Provincial Key Laboratory of Photonics Technology, Key Laboratory of Optoelectronic Science and Technology for Medicine of Ministry of Education, Fujian Normal University, China, and Guangzhou Qianmao Electronic Technology Co. Ltd, China.

REFERENCES

[1] L. Hong, Automatic personal identification using fingerprints. Michigan State University, 1998.
[2] K. W. Bowyer and M. J. Burge, Handbook of iris recognition. Springer, 2016.
[3] C. Ding, J. Choi, D. Tao, and L. S. Davis, "Multi-directional multi-level dual-cross patterns for robust face recognition," IEEE transactions on pattern analysis and machine intelligence, vol. 38, no. 3, pp. 518–531, 2016.
[4] T. Connie, M. K. O. Goh, and A. B. J. Teoh, "A grassmannian approach to address view change problem in gait recognition," IEEE transactions on cybernetics, vol. 47, no. 6, pp. 1395–1408, 2017.
[5] J. Zhang, J. Pu, C. Chen, and R. Fleischer, "Low-resolution gait recognition," IEEE Transactions on Systems, Man, and Cybernetics, Part B (Cybernetics), vol. 40, no. 4, pp. 986–996, 2010.
[6] D. Dubin, Rapid Interpretation of EKG's. USA: Cover Publishing Company, 1996, 1996.

[7] L. Biel, O. Pettersson, L. Philipson, and P. Wide, "Ecg analysis: a new approach in human identification," IEEE Transactions on Instrumentation and Measurement, vol. 50, no. 3, pp. 808–812, 2001.
[8] X. Fan, Q. Yao, Y. Cai, F. Miao, F. Sun, and Y. Li, "Multiscaled fusion of deep convolutional neural networks for screening atrial fibrillation from single lead short ecg recordings," IEEE journal of biomedical and health informatics, vol. 22, no. 6, pp. 1744–1753, 2018.
[9] D. Deuchar, "Ballistocardiography." British heart journal, vol. 29, no. 3, p. 285, 1967.
[10] U. S. N. Aeronautics, S. A. Scientific, T. I. Division, and U. S. F. A. Agency, "Ballistocardiography : a bibliography," 1965, "FAA AM 65-15.".
[11] H. Guo, X. Cao, J. Wu, and J. Tang, "Ballistocardiogram-based person identification using correlation analysis," in World Congress on Medical Physics and Biomedical Engineering May 26-31, 2012, Beijing, China. Springer, 2013, pp. 570–573.
[12] F. G. Baptista, D. E. Budoya, V. A. de Almeida, and J. A. C. Ulson, "An experimental study on the effect of temperature on piezoelectric sensors for impedance-based structural health monitoring," Sensors, vol. 14, no. 1, pp. 1208–1227, 2014.
[13] P. Wei, X. Han, D. Xia, T. Liu, and H. Lang, "Novel fiber-optic ring acoustic emission sensor," Sensors, vol. 18, no. 1, p. 215, 2018.
[14] Z. Sun, B. Rocha, K.-T. Wu, and N. Mrad, "A methodological review of piezoelectric based acoustic wave generation and detection techniques for structural health monitoring," International Journal of Aerospace Engineering, vol. 2013, 2013.
[15] Q. Zhang, D. Zhou, and X. Zeng, "Heartid: a multiresolution convolutional neural network for ecg-based biometric human identification in smart health applications," IEEE Access, vol. 5, pp. 11 805–11 816, 2017.
[16] Y. N. Singh and S. K. Singh, "A taxonomy of biometric system vulnerabilities and defences," International journal of biometrics, vol. 5, no. 2, pp. 137–159, 2013.
[17] M. Komeili, W. Louis, N. Armanfard, and D. Hatzinakos, "On evaluating human recognition using electrocardiogram signals: From rest to exercise," in Electrical and Computer Engineering (CCECE), 2016 IEEE Canadian Conference on. IEEE, 2016, pp. 1–4.
[18] S. A. Israel, J. M. Irvine, A. Cheng, M. D. Wiederhold, and B. K. Wiederhold, "Ecg to identify individuals," Pattern recognition, vol. 38, no. 1, pp. 133–142, 2005.
[19] L. Kanaan, D. Merheb, M. Kallas, C. Francis, H. Amoud, and P. Honeine, "Pca and kpca of ecg signals with binary svm classification," in Signal Processing Systems (SiPS), 2011 IEEE Workshop on. IEEE, 2011, pp. 344–348.
[20] Q. Zhang and D. Zhou, "Deep arm/ear-ecg image learning for highly wearable biometric human identification," Annals of biomedical engineering, vol. 46, no. 1, pp. 122–134, 2018.
[21] Y. Zhang, Z. Chen, and H. I. Hee, "Noninvasive measurement of heart rate and respiratory rate for perioperative infants," Journal of Lightwave Technology, 2018.
[22] Z. Chen, D. Lau, J. T. Teo, S. H. Ng, X. Yang, and P. L. Kei, "Simultaneous measurement of breathing rate and heart rate using a microbend multimode fiber optic sensor," Journal of biomedical optics, vol. 19, no. 5, p. 057001, 2014.
[23] J. Shin, B. Choi, Y. Lim, D. Jeong, and K. Park, "Automatic ballistocardiogram (bcg) beat detection using a template matching approach," in Engineering in Medicine and Biology Society, 2008. EMBS 2008. 30th Annual International Conference of the IEEE. IEEE, 2008, pp. 1144–1146.
[24] H. J. Baek, G. S. Chung, K. K. Kim, and K. S. Park, "A smart health monitoring chair for nonintrusive measurement of biological signals," IEEE transactions on Information Technology in Biomedicine, vol. 16, no. 1, pp. 150–158, 2012.
[25] C.-W. Hsu and C.-J. Lin, "A comparison of methods for multiclass support vector machines," IEEE transactions on Neural Networks, vol. 13, no. 2, pp. 415–425, 2002.
[26] M. D. Zeiler and R. Fergus, "Visualizing and understanding convolutional networks," in European conference on computer vision. Springer, 2014, pp. 818–833.
[27] P. Murugan, "Feed forward and backward run in deep convolution neural network," arXiv preprint arXiv:1711.03278, 2017.
[28] G. Grinstein, M. Trutschl, and U. Cvek, "High-dimensional visualizations," in Proceedings of the Visual Data Mining Workshop, KDD, 2001.
[29] C.-C. Chang and C.-J. Lin, "LIBSVM: A library for support vector machines," ACM Transactions on Intelligent Systems and Technology, vol. 2, pp. 27:1–27:27, 2011, software available at http://www.csie.ntu.edu.tw/ cjlin/libsvm.

YI ZHANG was born in Quanzhou, Fujian, China. He received his B.S. degree in software engineering from Software College, Xiamen University (XMU), China, in 2014. He received his M.S. degree from Graduate Institute of Communication Engineering (GICE), National Taiwan University (NTU), Taipei, Taiwan, in 2016. His primary research areas include wireless communication, game theory, optimization and signal processing.

ZHIHAO CHEN received the B.Sc. degree from East China Normal University, the M.Sc. degree from Shanghai University of Science and Technology, and the Ph.D. from Tsinghua University, China, respectively. From 1998 to 1999, he was with the City University of Hong Kong and then joined Nanyang Technological University, Singapore, as research fellow. From 2001 to 2004 he was a member of technical staff with Oluma Inc, USA. From 2004 to 2016, he was Senior Scientist with Institute for Infocomm Research, Singapore where he was working on fiber sensors for healthcare and other industrial applications. Now he is professor at Quanzhou Normal University, China, where his research interests include optical fiber sensors and lasers for biomedical and industrial applications. He has authored and co-authored more than 120 papers in journals and conferences. As inventor and co-inventor, he has 8 US, China and Singapore patents granted and a few pending.

WEIJUAN CHEN was born in Fujian, China, in February 1993. She was the student of College of Photonic and Electronic Engineering, Fujian Normal University, China, where she is currently studying for a Ph.D. degree.And now she is working for professor Zhihao Chen's team at Quanzhou Normal University.Her research interests include fiber optical humidity sensors, PH sensors and interferometer sensors.

HUI LI received the B.Sc. degree from Peking University, the M.Sc. degree in optics from Fujian Normal University, and the Ph.D. in optical engineering from Zhejiang University, China, respectively. For more than 20 years his research interests have included biological tissue optics, photoacoustic imaging and optical coherence tomography and their applications, and so on. He has authored and co-authored more than 130 papers in journals and conferences.